Indian J. Phys. **78A** (1), 53-55 (2004)

Nanomaterials–2003

AN INTERNATIONAL JOURNAL
IJP A

Conventional ceramic route for the production of nanocrystalline ferrites

T K Kundu* and D Chakravorty#

*Department of Physics and Technophysics, Vidyasagar University, Midnapore-721 102, West Bengal, India

Indian Association for the Cultivation of Science, Jadavpur, Kolkata-700 032, India

Abstract · Niobium (Nb^{5+}) ion doped manganese ferrites ($MnFe_2O_4$) and manganese-zinc ferrites $(MnZn)Fe_2O_4$ are developed by the conventional ceramic route. Nanostructured particles are found to evolve with increasing dopant concentration. Formation of nanoscale domains of ferrite is evident from the study of transmission electron micrographs. Typically the minimum size of the grain in Nb^{5+} doped $MnFe_2O_4$ lies in the range of 13 7 nm. Magnetic parameters like Curie temperature and Coercive field show a strong dependence on the size of the ferrite grains. It is concluded that the aliovalent ions break up the ferromagnetically active oxygen polyhedra and the sizes of the grains are reduced.

Keywords Nanoferrites, $MnFe_2O_4$, nanostructured magnetic materials.

PACS Nos. : 75.50.Tt, 68.37.Lp, 81.07.-b

1. Introduction

Nanoscale spinel ferrites have drawn a large attention because of their technological importance in magnetic recording, magnetic fluids and catalyst. Moreover, from a more fundamental point of view, the peculiar magnetic properties of the nanoscale ferrite particles have been of particular interest for a long time. A variety of methods have been reported for the synthesis of nanocrystalline ferrites like co-precipitation, co-sputtering, citrate precursor *etc* [1-3]. But neither of the methods is so useful for the production of nano-ferrites in mass scale. We explored the conventional ceramic route for the production of nanocrystalline spinel ferrites with suitable doping by aliovalent ions.

Effects of lanthanum impurities on the microstructure and property changes have previously been reported for ferroelectric PZT phase [4, 5]. It was found that the doping of aliovalent ions could suppress the long-range ferroelectric order in the system. Thus nanostructure phase was found to induce with increasing La impurity content in the ferroelectric ceramic system. The results are explained in terms of generation of vacancies in some cation sites that appears to destroy the long-range order and form nanostructured ferroelectrics [6]. A similar approach is taken in the present case to prepare a set of nanocrystalline spinel ferrites.

* Corresponding Author

2. Nanostructured $MnFe_2O_4$

The materials had a target composition represented by xNb_2O_5, $(0.5\text{-}x)$ $MnO, 0.5Fe_2O_3$ with x having values 0. 0.05, 0.10, 0.15 and 0.20 respectively. The specimen with the above target composition was made from starting materials $MnCO_3$, Fe_2O_3, and Nb_2O_5. Required amount of staring materials was taken in a mortar and mixed for duration of 2–3 h under acetone. The powder was then calcined at 800°C for 2 h for the nucleation of the magnetic phase. The calcined powder was pressed into pellet by the cold isotatic pressing method with a pressure of 5 bars for 5 minutes. The pellets were sintered at 1000°C for 2°h. The structure of the sample was analyzed by X-ray diffraction with a Rich Seifert 3000P X-ray diffractometer with filtered CuK_α radiation of wavelength λ = 0.15405 nm. Average value of D was calculated from widths, $\Delta 2\theta_{1/2}$, in the X-ray diffraction

Table 1. Summary of particle diameters in the $MnFe_2O_4$ samples

Specimen No.	The value of x	Particle diameter from XRD	Particle diameter From TEM
1	0.00	1 μm	1 μm
2	0.05	95 nm	100 nm
3	0.10	35.5 nm	41.0 nm
4	0.15	16.7 nm	20.5 nm
5	0.20	14.2 nm	13.7 nm

peaks with the Debye Scherrer relation [7]. Its microstructure was studied with a JEM 200CX transmission electron microscope and the magnetic measurement were carried out with a PAR vibrating sample magnetometer.

X-ray diffraction patterns show that the specimens consist of $MnFe_2O_4$ and $(MnFe)_2O_3$ with volume fraction of two phases to be around 0.49 and about 0.51 respectively as estimated from their most intense line. The grain size of the crystallites was primarily estimated from the broadening of most intense X-ray line for $MnFe_2O_4$ by using Scherrer formula

$$D = \frac{0.9\lambda}{\beta \cos\theta}$$

where D is the diameter of the grain, β is FWHM in the X-ray diffraction peak, λ is the wavelength and θ is the angle of diffraction. The particle diameters calculated from the above formula are summarized in Table 1. The grain size in specimen 1 remains in the range of micrometer. With the doping of Nb_2O_5, the size of $MnFe_2O_4$ is reduced down to 13.7 nm.

The results obtained from X-ray broadening are in reasonable agreement with those determined by transmission electron microscopy. Figure 1(a) shows a typical TEM picture for specimen 4 and the corresponding diffraction ring pattern is shown in Figure 1(b). The interplanar spacing was calculated from the diameter of the rings and it confirms the presence of $MnFe_2O_4$ in the system. Since the ionic radius of Nb^{5+} (0.07 nm) is quite close to that of Mn^{2+}, Nb^{5+} will substitute the Mn^{2+} sites with the creation of vacancy. The presence of Nb^{5+} ions and the resultant vacancies are believed to break the coupling of ferrimegnetically active oxygen polyhedra. Magnetization *versus* field for the sample was taken at temperatures ranging from 300 K to 570 K. A typical such plot for sample no 5 at room temperature is shown in Figure 2.

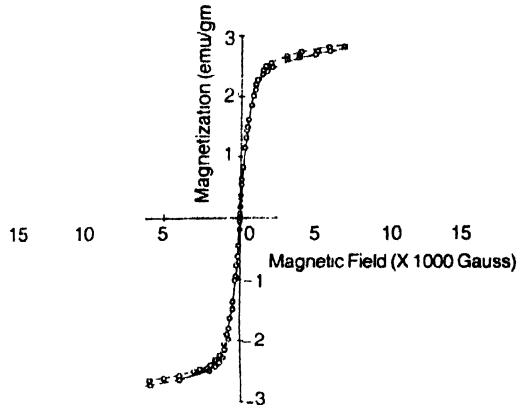

Figure 2. Magnetization *vs* field for specimen 5 at room temperature

Table 2. Summary of magnetic properties of the $MnFe_2O_4$ samples.

Specimen No.	Saturation magnetization (emu/gm)	Coercive field	Curie temperature
1	42	1.0 G	556 K
2	27	2.0 G	545 K
3	20	2.0 G	533 K
4	11	5.0 G	531 K
5	3	25.5 G	534 K

Figure 1(a). Transmission Electron Micrograph for specimen 4.

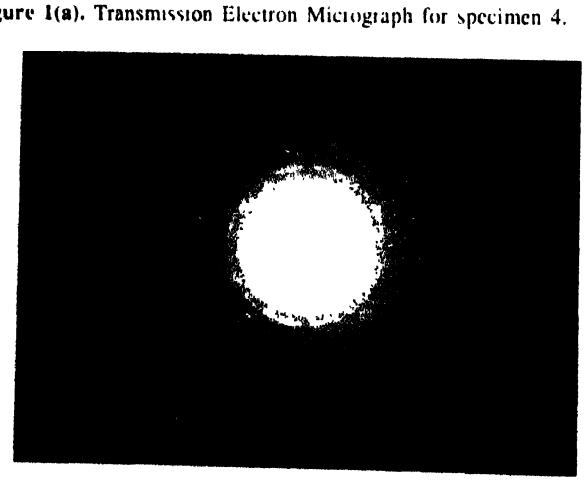

Figure 1(b). Electron Diffraction rings for specimen 4

The results of room temperature saturation magnetization and coercivity as a function of particle diameter are given in Table 2. The estimated values of saturation magnetizations vary linearly with the inverse diameter of the $MnFe_2O_4$ phase. This behaviour can be explained introducing core-shell model of magnetic nanoparticles [8]. In the present case the shell, made of Nb^{5+} doped $MnFe_2O_4$ materials, has smaller magnetization compared to the core. Tabulated values of H_c show that it increases from 2 to 25G as the particle diameter of $MnFe_2O_4$ is decreased from 100 nm to 13.7 nm. Theoretical reports predicted that for magnetic nanoparticles coercivity H_c depend inversely on magnetization [9-10]. Therefore this behaviour of H_c may be explained in terms of the variation of saturation magnetization as a function of particle diameter as discussed earlier.

The last column of Table 2 shows the values of Curie temperature in the systems. The measurement was carried out with an applied filed of 10 G. Curie temperature decreases from 556 K to 530 K with the decrease of particle diameter of $MnFe_2O_4$ to 13.7 nm. This is consistent with the earlier reports [11–12]. As

discussed in the previous section that Nb^{5+} substitutes the Mn^{2+} sites, number of pair of Mn^{2+}-Fe^{3+} ions giving exchange interaction is lowered with the increase of Nb_2O_5 content. Thus a lowering of T_c with the decrease of particle diameter of $MnFe_2O_4$ is observed in the present case.

3. Nanostructured (MnZn)Fe_2O_4

Nanostructured (MnZn)Fe_2O_4 materials were generated using a similar approach as that of $MnFe_2O_4$. The target composition was $x$$Nb_2O_5$, (0.5-$x$)/2 MnO, (0.5-$x$)/2 ZnO 0.5$Fe_2O_3$ with x having values 0.0, 0.10, 0.20 and 0.25 respectively. The final (MnZn)Fe_2O_4 magnetic materials in the form of pellets were developed by using the same experimental procedure as discussed in the previous section. Crystalline phase precipitated in the specimen and the grain size of the crystal were estimated from X-ray diffractogram. Magnetic properties were carried out at room temperature using PAR vibrating sample magnetometer.

X-Ray diffractograms show the presence of single phase of (MnZn)Fe_2O_4 in the samples. The diameter of (MnZn)Fe_2O_4 lies in the range of nanometer. The lowest diameter of 50 nm is generated with 25 mol% Nb_2O_5 doping. It is observed that the size of (MnZn)Fe_2O_4 grain gradually decreases with the increase of Nb5' content as summarized in Table 3. Magnetic measurement shows that M_s decreases and H_c increases with the decrease of (MnZn)Fe_2O_4 diameter.

Table 3. Summary of particle diameter and magnetic properties of the (MnZn)Fe_2O_4.

Specimen No	The value of x	Particle diameter From XRD	Saturation magnetization (emu/gm)
a	0.00	1 μm	12
b	0.10	150 nm	6
c	0.20	72 nm	2
d	0.25	50 nm	1

The behaviour shown above is similar in nature to the previous results of nanostrauctured $MnFe_2O_4$ and therefore identical explanation is valid for (MnZn)Fe_2O_4 . These experimental results support the mechanism discussed above for the formation of nanostructured materials by aliovalent ion doping.

4. Summary

Nano-sized particles of manganese ferrites ($MnFe_2O_4$) and manganese-zinc ferrites (MnZn)Fe_2O_4 are developed by the conventional ceramic route using doping with aliovalent (Nb^{5+}) ions. Particle diameters are found to decrease with increasing dopant content. Magnetic parameters depend strongly on the size of the ferrite grains. These are explained in terms of the substitution of Nb^{5+} ions in the Mn^{2+} or Zn^{2+} sites. The substitution of Nb^{5+} ions essentially break up the ferromagnetically active oxygen polyhedra and the sizes of the grains are reduced.

Acknowledgment

The work is supported by a project of Department of Science and Technology, Government of India, New Delhi (No.100/IFD/3567/2002-03).

References

[1] M Ferele and K Baberschke *Phys Rev Lett* **58** 511 (1987)

[2] X Tang, C M Sorensen and K J Klabunde *Phys Rev. Lett.* **67** 3602 (1991)

[3] A Chatterjee, D Das, S K Pradhan and D Chakravorty, *J. Magn Magn Mater.* **127** 214 (1993)

[4] J E Li, X Dai, A Chow and D Viehland *J Mater Res.* **10** 926 (1995)

[5] Z Xu, X Dai and D Viehland *Phys. Rev.* **B51** 6261 (1995)

[6] Z Xu, X Dai J F Li and D Viehland *Appl Phys Lett* **68** 1628 (1996)

[7] L Azaroff *Elements of X-ray Crystallography* (New York . McGraw-Hill) p557 (1968)

[8] T Sato, T Iijima, M Seki and N Inagaki *J. Magn. Magn Mater* **65** 252 (1987)

[9] F H Feri, S Shtrikman and D Treves *Phys. Rev.* **106** 446 (1957)

[10] E F Kneller and E F Luborsky *J. Appl Phys.* **34** 656 (1963)

[11] M Stampanoni, A Vaterlans, M Aeschlimann and F Meier *Phys Rev Lett* **59** 2483 (1987)

[12] C M Schneider, P Bressler, P Schuster and J Kirchner *Phys. Rev Lett.* **64** 1059 (1990)